

Weakly-Supervised Action Localization with Expectation-Maximization Multi-Instance Learning

Zhekun Luo¹ Devin Guillory¹ Baifeng Shi² Wei Ke³ Fang Wan⁴
Trevor Darrell¹ Huijuan Xu¹

¹University of California, Berkeley ²Peking University

³Carnegie Mellon University ⁴Chinese Academy of Sciences

¹{zhekun_luo, dguillory, trevordarrell, huijuan}@eecs.berkeley.edu,
²bfshi@pku.edu.cn, ³weik@andrew.cmu.edu, ⁴wanfang@ucas.ac.cn

Abstract. Weakly-supervised action localization problem requires training a model to localize the action segments in the video given only video level action label. It can be solved under the Multiple Instance Learning (MIL) framework, where a bag (video) contains multiple instances (action segments). Since only the bag’s label is known, the main challenge is to assign which key instances within the bag trigger the bag’s label. Most previous models use an attention-based approach. These models use attention to generate bag’s representation from instances and then train it via bag’s classification. In this work, we explicitly model the key instances assignment as a hidden variable and adopt an Expectation-Maximization framework. We derive two pseudo-label generation schemes to model the E and M process and iteratively optimize the likelihood lower bound. We also show that previous attention-based models implicitly violate the MIL assumptions that instances in negative bags should be uniformly negative. In comparison, Our EM-MIL approach more accurately models these assumptions. Our model achieves state-of-the-art performance on two standard benchmarks, THUMOS14 and ActivityNet1.2, and shows the superiority of detecting relative complete action boundary in videos containing multiple actions.

Keywords: weakly-supervised learning, action localization, multiple instance learning

1 Introduction

As the growth of video content accelerates, it becomes increasingly necessary to improve the video understanding ability with less annotation effort. The cost of annotating what action occurs in a video, as well identifying exactly where in the video this action happens, is high in comparison with the cost of whole video labeling since videos can contain several hundreds or thousands of frames. In addition, the exact start and stop points of an action are often subjective [10]. As such, researchers are motivated to explore approaches that require less annotations. In this work, we focus on weakly-supervised temporal activity detection

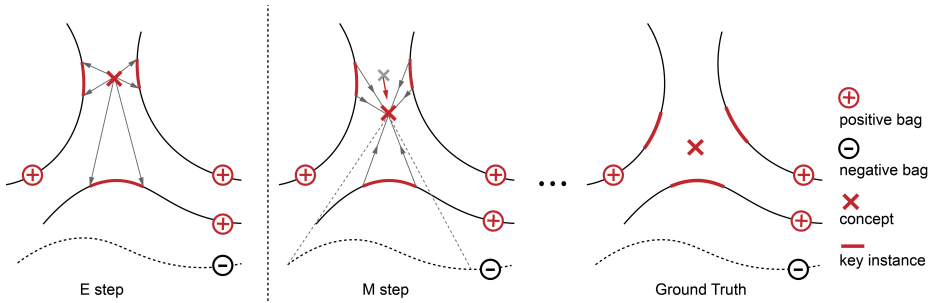


Fig. 1: Every line represents a bag, and the points on the line represent instances within the bag. We aim to find a concept point in this feature space such that each positive bag contains some key instances close to it while every instance in the negative bags is far from it. In E step we use the current concept to pick key instances from each positive bag. Then in M step we uses these key instances and negative bags to update the concept.

paradigm, using only video level class labels to learn activity recognition and localization. These weakly-supervised models can significantly reduce the annotation effort, and have the additional benefit that existing search engines could be leveraged to generate annotations.

The weakly-supervised activity detection problem can be framed as a special case of the **Multiple Instance Learning (MIL)** problem [7]. In the binary MIL setting, a bag’s label is positive if at least one instance in the bag is positive. Therefore a bag is negative only if all instances in the bag are negative. In our task, each video represents a bag, and the clips of the video represent instances inside the bag. Only the bag’s label is available during training time, and the main goal is to learn a model to classify instances’ label. The key challenge here is to handle **key instance assignment** during training – to identify which instances within the bag trigger the bag’s label.

Most of the previous models solving this problem used an **attention-based** approach to model the key instance assignment process. [12] outlines a generalized framework for these models. They used attention weights to combine instance-level class prediction to produce the bag’s classification result. Models of this form are then trained via standard classification procedures. The learned attention weights imply the contribution of each instance to the bag’s label, and thus can be used to localize the positive instances (action segments). Untrimmed-Net [33] and [21] are two prominent examples of this approach. Various regularizations have been added to this base framework [24,20,22,17]. While promising results have been observed, models of this variety tend to produce incomplete action proposals as discussed in [38,17], which is also a common problem for attention-based models used in weakly-supervised object detection [32,15]. We define completeness of an action proposal as its temporal coverage of the ground truth action region. It is related to reducing false negatives. Incomplete propos-

als indicate that the model only detects part of the action and can be verified by high IoU metric scores.

We adopt a different approach using the ExpectationMaximization framework. Historically, ExpectationMaximization (EM) or similar iterative estimation processes have been used to solve the MIL-learning problems [42,7,8] before deep learning era. These models frame the MIL-objective as to find a **concept** in the feature space such that every positive bag contains at least one instance that is close to the concept, while all instances in negative bags are far from it. [42] explicitly models the instance assignment as a hidden variable and selects one key instance per bag. The optimization is done by iterative reassignment of the concept (M step) and key instances (E step).

These traditional methods are typically applied in much simpler settings but they give us some clear intuition. The previous attention-based framework is comprised by two interdependent steps. If we have a perfect per clip classification model, then the correct attention score can be induced on clips with high classification score, and vice versa. High attention weights directly correspond to action regions, and thus attention score is exactly our optimization target. But in an attention-based framework, attention is learned as a by-product when doing classification for bags. As a result, the attention module tends to only pick the most discriminative parts of the action or objects to correctly classify a bag, since the loss and training signal come from the bag’s classification result.

Instead, we explicitly model key instance assignment as a hidden variable and optimize for this as our target. We adopt the ExpectationMaximization algorithm to solve the interlocking steps of key instance assignment and action concept classification. For video tasks, we cannot select one key instance per bag because an action usually contains multiple clips. We therefore extend the definition of key instance to the **key instance scope** defined in Sec 3.1. We parametrize the model using contemporary convolutional neural network architectures. To formulate our learning objective, we derive two pseudo-label generating schemes to model the E and M process respectively. We show that our alternating update process optimizes a lower bound of the MIL-objective. A high level diagram for our motivation is in figure 1.

We compare our model with previous attention-based approaches. We find that previous models implicitly violate the MIL assumptions. They apply attention to negative bags, while the MIL assumption states that instances in negative bags are uniformly negative. We show that our method can better model the data generating procedure of both positive and negative bags and achieves better temporal localization performance.

In addition, one strength of our model is its simplicity: it requires only EM plus pseudo-labeling and a contemporary network architecture to achieve strong result. There is no auxiliary losses or temporal constraint unlike [24,17,38]; our method’s simplicity suggests the potential of the framework to be extended to many practical settings. The main contributions of this paper are:

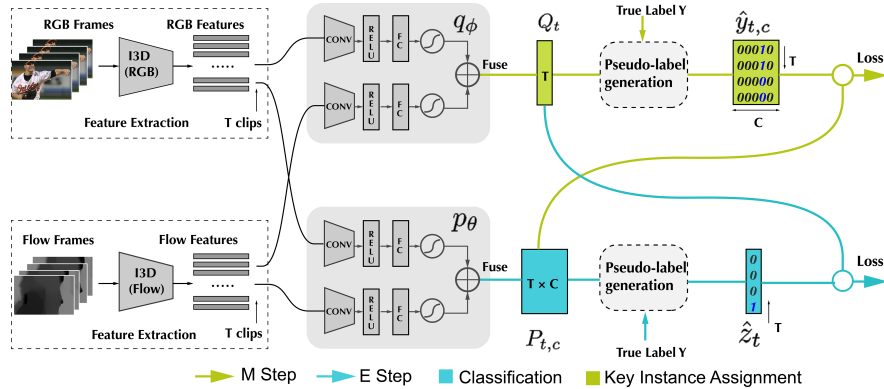


Fig. 2: Our EM-MIL model architecture, which builds on two-stream I3D features and alternates between updating the key-instance assignment branch q_ϕ (E Step) and the classification branch p_θ (M Step). We use the classification score and key instance assignment result to generate pseudo-labels for each other (detailed in Sec. 3.1 and Sec. 3.2), and alternate freezing one branch to train the other.

- We propose to adapt the ExpectationMaximization MIL framework to weakly supervised action localization task. We derive two novel pseudo-label generating schemes to model the E and M process respectively.
- We show that previous attention-based MIL methods implicitly violate the MIL assumptions. In comparison, our method can better model the foreground and background information.
- Our model is evaluated on two standard benchmarks, THUMOS14 and ActivityNet1.2, and achieves state of the art results. In particular, we show empirically that our EM process is more robust and produce action proposals that are more complete in videos with multiple actions.

2 Related Work

Weakly-Supervised Action Localization Weakly supervised action localization learns to localize activities inside videos when only action class labels are available. UntrimmedNet [33] first used attention to model the contribution of each clip to a video’s global action label. It performs classification separately at each clip, and predicts video’s label through a weighted combination of clips’ scores. Later the STPN model [21] proposed that instead of combining clips’ scores, it uses attention to combine each clip’s feature into a bag-level feature vector and conducts classification from there. [12] generalizes a framework for these attention-based approaches and formalizes such combination as a permutation-invariant aggregation function. W-TALC [24] proposed a regularization to enforce action regions of the same class must share similar features. People soon noticed that these models tend to produce incomplete results. To

tackle that, a series of papers [28,29,45,40] took the adversarial erasing idea to improve the detection completeness by hiding the most discriminative parts. [38] conducted sub-samplings based on activation to suppress the dominant response of the discriminative action regions. To model complete actions, [17] proposed to use a multi-branch network with each branch handling distinctive action parts.

The above models combine per-clip attention and classification scores to form the Temporal Class Activation Sequence (T-CAS, defined in [21]) and then group the high activation clips to generate action proposals. Instead of post-grouping, AutoLoc [26] trains a boundary predictor using the high T-CAS activation regions of a pre-trained UntrimmedNet[33] as ground truth. In this way, the model can directly output the action start and end point without grouping, and Clean-Net [18] follows a similar pipeline.

It is worth noting that, some previous methods in weakly supervised object or action localization involve iterative refinement, but their training processes and objectives are different from our ExpectationMaximization method. RefineLoc[2]’s training contains several passes. It uses the result of the i_{th} pass as supervision for the $(i+1)_{th}$ pass and trains a new model from scratch iteratively. [31] uses a similar approach in image objection detection but stacks all passes together. Our approach differs from these in the following ways: First, their self-supervision and iterative refinement happen between **different passes**, but in each pass all modules are trained jointly till converge. In comparison, we adopts an EM framework which explicitly models key instance assignment as hidden variables. Our pseudo-labeling and alternating training happen between **different modules** of the same model. As a result, our model requires only one pass. In addition, as discussed in section 3.4 , they handle the attention in negative bags and background instances different to us.

Classic Multiple Instance Learning Methods The Multiple Instance Learning problem was first defined by Dietterich et al [7], who proposed the iterated-discrimination algorithm. It starts from a point in the feature space and iteratively searches for the smallest box covering at least one point (instance) per positive bag avoiding all points in negative bags. [19] sets up a framework to solve this problem called Diverse Density. They defined a point in the feature space to be the positive concept. Every positive bag (“diverse”) contains at least one instance close to the concept while all instances in the negative bags are far from it (in terms of some distance metric). They then modeled the likelihood of a concept using Gaussian Mixture models along with a Noisy-OR probability estimation. [41] then applied AdaBoost to this Noisy-OR model and [14]’s ISR model, and derived two different MIL loss functions. [8] adapted the K-nearest neighbors algorithm to the Diverse Density framework. Later [42] proposed the EM-DD algorithm, combing Expectation Maximization process and the Diverse Density metric. Many of these early works involve modeling key instances assignment as hidden variable and use iterative optimization to search for the best assignment, which is a direct inspiration for our proposed model.

3 Method

Suppose we have a set of videos and their corresponding video-level labels. Each video (bag) contains T video clips (instances), denoted by $\mathbf{X} = \{\mathbf{x}_t\}_{t=1}^T$, where $\mathbf{x}_t \in \mathbb{R}^d$ is the feature of clip t . We represent the video’s action label in one hot way, where $y_c = 1$ if the video contains clips of action c , otherwise $y_c = 0$, $c \in \{1, 2, \dots, C\}$. In the MIL setting, label of each video is determined by the label of clips it contains. To be specific, we assign a binary variable $z_t \in \{0, 1\}$ to each clip t , denoting whether clip t is responsible for the generation of video-level label. \mathbf{z} models the assignment of **key instances scope**. Given $\mathbf{z} = \{z_t\}_{t=1}^T$, video-level label is generated with probability

$$p_\theta(y_c = 1 | \mathbf{X}, \mathbf{z}) = \sigma_{t \in \{1, \dots, T\}} \{ p_\theta(y_{c,t} = 1 | \mathbf{x}_t) \cdot [z_t = 1] \}, \quad (1)$$

where $p_\theta(y_{c,t} = 1 | \mathbf{x}_t)$ is the probability (parameterized by θ) that clip t belongs to class c . The closer clip t is to the concept, the higher $p_\theta(y_{c,t} = 1 | \mathbf{x}_t)$ is. σ is a permutation-invariant operator, *e.g.* maximum operator [43] or mean operator [12].

In our temporal action localization problem, we propose to first estimate the probability of $z_t = 1$ with an estimator $q_\phi(z_t = 1 | \mathbf{x}_t)$ parameterized by ϕ , and then choose the clips with high estimated likelihood as our action regions. Since $\{z_t\}$ are latent variables with no ground truth, we optimize q_ϕ through maximization of the variational lower bound:

$$\begin{aligned} \log p_\theta(y_c | \mathbf{X}) &= KL(q_\phi(\mathbf{z} | \mathbf{X}) \parallel p_\theta(\mathbf{z} | \mathbf{X}, y_c)) + \int q_\phi(\mathbf{z} | \mathbf{X}) \log \frac{p_\theta(\mathbf{z}, y_c | \mathbf{X})}{q_\phi(\mathbf{z} | \mathbf{X})} d\mathbf{z} \\ &\geq \int q_\phi(\mathbf{z} | \mathbf{X}) \log p_\theta(\mathbf{z}, y_c | \mathbf{X}) d\mathbf{z} + H(q_\phi(\mathbf{z} | \mathbf{X})), \end{aligned} \quad (2)$$

where $H(q_\phi(\mathbf{z} | \mathbf{X}))$ is entropy of q_ϕ . By maximizing the lower bound, we are actually optimizing the likelihood of y_c given \mathbf{X} . In this work, we adopt the Expectation-Maximization (EM) algorithm, and optimize the lower bound by updating θ and ϕ alternately. To be specific, we first update ϕ by minimizing $KL(q_\phi(\mathbf{z} | \mathbf{X}) \parallel p_\theta(\mathbf{z} | \mathbf{X}, y_c))$ and tighten the lower bound in E step, and update θ through maximization of the lower bound in M step. In the following subsections, we will first get into details of updating θ and ϕ in E and M step separately, and then sum up the whole algorithm.

3.1 E Step

In E step, we update ϕ by minimizing $KL(q_\phi(\mathbf{z} | \mathbf{X}) \parallel p_\theta(\mathbf{z} | \mathbf{X}, y_c))$ and tighten the lower bound in Eq. 2. As in previous works [21, 22], we approximate $q_\phi(\mathbf{z} | \mathbf{X})$ with $\prod_t q_\phi(z_t | \mathbf{x}_t)$ assuming independence between different clips, where $q_\phi(z_t | \mathbf{x}_t)$ is estimated by neural network with parameter ϕ on each clip. Thus we only have to minimize $KL(q_\phi(z_t | \mathbf{x}_t) \parallel p_\theta(z_t | \mathbf{x}_t, y_c))$ for each clip t . Following the literature, we assume that the posterior $p_\theta(z_t | \mathbf{x}_t, y_c)$ is proportional to the classification score $p_\theta(y_c | \mathbf{x}_t)$. Then we propose to update q_ϕ with pseudo label generated from

classification score. Specifically, dynamic thresholds are calculated based on the instance classification scores to generate pseudo-labels for q_ϕ . If an instance has a classification score over the threshold for any ground truth class within the video, the instance is treated as a positive example; otherwise, it is treated as a negative example. The pseudo label is formulated as follows:

$$\hat{z}_t = \begin{cases} 1, & \text{if } \sum_{c=1}^C \mathbb{1}(P_{t,c} > \bar{P}_{1:T,c} \wedge y_c = 1) > 0 \\ 0, & \text{otherwise} \end{cases} \quad (3)$$

where $P_{t,c} = p_\theta(y_c|\mathbf{x}_t)$ and $\bar{P}_{1:T,c}$ is the mean of $P_{t,c}$ over temporal axis. Then we update q_ϕ using binary cross entropy (BCE) loss and the updating process is illustrated in Fig. 4.

$$\mathcal{L}(q_\phi) = -\hat{z}_t \log q_\phi(z_t|\mathbf{x}_t) - (1 - \hat{z}_t) \log(1 - q_\phi(z_t|\mathbf{x}_t)). \quad (4)$$

3.2 M Step

In M step, we update p_θ through optimization of the lower bound in Eq. 2. Since $H(q_\phi(\mathbf{z}|\mathbf{X}))$ is constant wrt θ , we only optimize $\int q_\phi(\mathbf{z}|\mathbf{X}) \log p_\theta(\mathbf{z}, y_c|\mathbf{X}) d\mathbf{z}$, which is equivalent to optimize the classification performance given key instance assignment $q_\phi(\mathbf{z}|\mathbf{X})$. To this end, we use the class-agnostic key-instance assigning module q_ϕ and the ground truth video-level labels to generate a $T \times C$ pseudo-label map which discriminates between foreground and background clips within the same video. Similarly, our pseudo-label generation procedure calculates a dynamic threshold based on the distribution of instance-assignment scores for each video clip. It assigns ground truth classifications for all instances whose score is higher than the threshold and background classifications for all instances whose score is below or instances in negative bags. The pseudo label is given by:

$$\hat{y}_{t,c} = \begin{cases} 1, & \text{if } y_c = 1 \text{ and } Q_t > \bar{Q}_{1:T} + \gamma \cdot (\max(Q_t) - \min(Q_t)) \\ 0, & \text{otherwise} \end{cases}, \quad (5)$$

where $Q_t = q_\phi(z_t|\mathbf{x}_t)$ and $\bar{Q}_{1:T}$ is the mean of Q_t over temporal axis. Then we update p_θ with BCE loss and the updating process is illustrated in Fig. 3.

$$\mathcal{L}(p_\theta) = -\hat{y}_{t,c} \log p_\theta(y_c|x_t) - (1 - \hat{y}_{t,c}) \log(1 - p_\theta(y_c|x_t)). \quad (6)$$

3.3 Overall Algorithm

Now we summarize our algorithm in Alg. 1. We adopt an EM-style algorithm and update the key-instance assigning module q_ϕ and classification module p_θ alternately. In E step, we freeze the classification module p_θ and update q_ϕ using pseudo labels from p_θ . Then in M step, we optimize classification based on q_ϕ . Two steps are progressed alternately to maximize the likelihood $\log p_\theta(y_c|\mathbf{X})$, and meanwhile optimize the localization results.

Algorithm 1: EM-MIL Weakly-Supervised Activity Localization

```

Initialization:
learning rate  $\beta$ , classification threshold  $\gamma$ 
classifier parameters  $\theta$ , attention parameters  $\phi$ 
while  $\theta, \phi$  has not converged do
  #Estep
  for  $(\mathbf{X}, y_c)$  in train set do
     $P_{t,c} \leftarrow p_\theta(y_c|\mathbf{x}_t)$ ;
     $\phi \leftarrow \phi - \beta \cdot \nabla_\phi \mathcal{L}(q_\phi)$ ;
  end
  #Mstep
  for  $(\mathbf{X}, y_c)$  in train set do
     $Q_t \leftarrow q_\phi(z_t|\mathbf{x}_t)$ ;
     $\theta \leftarrow \theta - \beta \cdot \nabla_\theta \mathcal{L}(p_\theta)$ ;
  end
end

```

3.4 Comparison with previous methods

After careful examination of Eq. 3 and Eq. 5, we find that our pseudo-labeling process Q_t and $\hat{y}_{t,c}$ can also be considered as a special kind of attention. Denote loss function by $Loss$, then in Eq. 5, the loss is calculated as:

$$Loss [p_\theta(\mathbf{y}|\mathbf{x}), \mathcal{F}(\mathbf{Q}, \mathbf{y})] \quad (7)$$

\mathcal{F} is the pseudo label generation function in Eq. 5, $\mathbf{Q}, \mathbf{y}, \mathbf{x}$ is the compact expression of Q_t, y_c, x_t . On the other hand, if we denote attention and classification score as \mathbf{a}, \mathbf{c} , the loss for a typical attention-based model is:

$$Loss [\sigma(\mathbf{c} \odot \mathbf{a}), \mathbf{y}] \quad (8)$$

Here σ is the aggregation operator discussed in [12], such as reduce_sum or reduce_max. Comparing Eq. 7 to Eq. 8, it is easy to see that they can be matched. $p_\theta(\mathbf{y}|\mathbf{x})$ is classification score (corresponds to \mathbf{c}), and \mathbf{Q} can be seen as special attention (corresponds to \mathbf{a}). In M step, it attends to the key instance it estimates. But compared to previous attention methods, Eq. 3 shows that this ‘‘attention’’ only happens in positive bags. We believe it better aligns with the MIL assumption, which says that all instances in negative bags are uniformly negative. Previous methods that applies attention to negative bags implicitly assumes that some instances are more negative than others. This violates the MIL assumption. The differences between our attention formulation and theirs are illustrated in Figure 3 and 4. In addition, in Eq. 5, this ‘‘attention’’ is a threshold-based hard attention. Clips below the threshold are classified as background with high confidence, while clips above it are weighted equally and re-scored in the next iteration. We initialize our training procedure by labeling

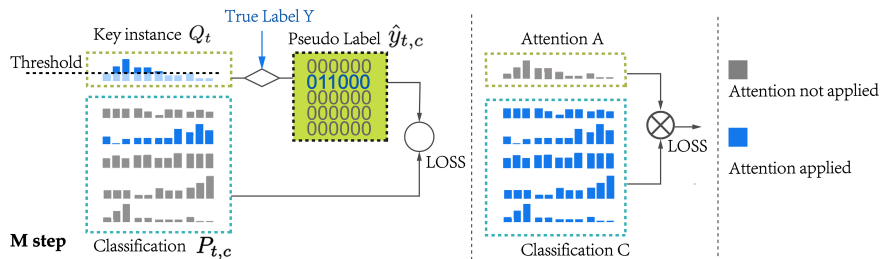


Fig. 3: Our EM-MIL model (left) uses key instance assignment Q_t to generate pseudo classification labels $\hat{y}_{t,c}$ only for the foreground classes, while in previous models such as UntrimmedNet (right) attentions are applied to all classes.

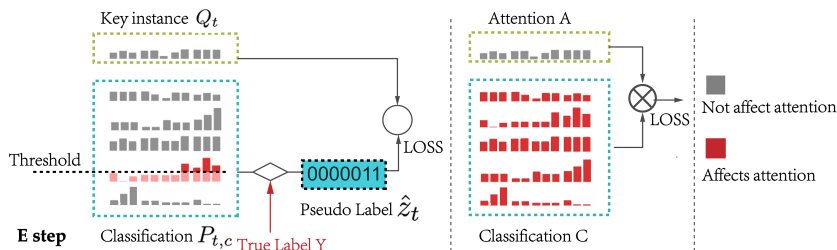


Fig. 4: In our EM-MIL model (left) only the foreground classification score $P_{t,c}$ affects the key instance pseudo label \hat{z}_t , while in previous models all-class classification scores contribute to the attention weights (right).

every clip in a positive bag to be 1 and gradually narrow down the search scope. Such training process maintains high recalls for action clips in each E-M iteration. It prevents attention from focusing on the discriminative parts too quickly, thus increases the proposal completeness.

3.5 Inference

At testing time, we use another branch for bag’s classification and use our model to get the score for localization as in previous work [26]. For classification branch, we used a plain UntrimmedNet [33] with soft attentions for the THUMOS14 dataset and the W-TALC [24] for the ActivityNet1.2 dataset. We run a forward pass with our model to get the localization score L by fusing instance assignment score Q_t and classification score $P_{t,c}$.

$$L_t = \lambda * Q_t + (1 - \lambda) * P_{t,c}, \quad (9)$$

where λ is set to be 0.8 through grid search in THUMOS14 dataset and 0.3 in the ActivityNet1.2 dataset. In the Experiment section 4.2 we find that the value difference of λ correlates with the underlying action distribution. We threshold the L_t score to get prediction y'_i for each clip using the same scheme as training time in Eq. 5. Then we group the clips above the threshold and convert them to get the start and end point of the action proposal.

4 Experiments

In this section, we evaluate our EM-MIL model on two large-scale temporal activity detection datasets: THUMOS14 [13] and ActivityNet1.2 [11]. Section 4.1 introduces experimental setup of the datasets, the evaluation metrics and the implementation details. Section 4.2 compares weakly localization results between our proposed model and the state-of-the-art models on both THUMOS14 and ActivityNet1.2 datasets, and visualize the localization results. Section 4.3 shows the ablation studies for each component of our model on THUMOS14 dataset.

4.1 Experimental Setup

Datasets: The THUMOS14 [13] activity detection dataset contains over 24 hours of videos from 20 different athletic activities. The train set contains 2765 trimmed videos, while the validation set and the test set contains 200 and 213 untrimmed videos respectively. We use the validation set as train data and report weakly-supervised temporal activity localization results on the test set. This dataset is particularly challenging as it consists of very long videos with multiple activity instances of very small duration. Most videos contain multiple activity instances of the same activity class. In addition, some videos contain activity instances from different classes.

The ActivityNet [11] dataset consists of untrimmed videos and is released in three versions. We use the ActivityNet1.2 dataset which contains a total of around 10000 videos including 4819 training videos, 2383 validation videos, and 2480 withheld testing videos for challenge purposes. We report the weakly-supervised temporal activity localization results on the validation videos. In ActivityNet1.2, over 99% videos contain activity instances of a single class. Many of the videos have activity instances covering more than half of the duration. Compared to THUMOS14, this is a large-scale dataset, both in terms of the number of activities involved and the amount of videos.

Evaluation Metric: The weakly-supervised temporal activity localization results are evaluated in terms of mean Average Precision (mAP) with different temporal Intersection over Union (tIoU) thresholds, which is denoted as $\text{mAP}@_\alpha$ where α is the threshold. Average mAP at 10 evenly distributed tIoU thresholds between 0.5 and 0.95 is also commonly used in the literature.

Implementation Details: Video frames are sampled at 12 fps (for THUMOS14) or 25 fps (for ActivityNet1.2). For each frame, we perform the center crop of size 224×224 after re-scaling the shorter dimension to 256 and construct video clip for every 15 frames. We extract the features of the clips using the publicly released, two-stream I3D model pretrained on Kinetics dataset [4]. We use the convolutional feature map of Mixed_5c layer for feature representation. For optical flow stream, TV-L1 flow [39,34] is used as the input.

Our model is implemented in pyTorch and trained using Adam optimizer with initial learning rate 0.0001 for both datasets. For the THUMOS14 dataset, we train the model alternating E/M step every 10 epochs in the first 30 epochs.

Table 1: Our EM-MIL detection results on THUMOS14 (in percentage). mAP at different IoU thresholds α are reported. The top half of the table shows performance from fully-supervised methods while the bottom half shows weakly-supervised models including ours.

Supervision	Models	α						
		0.1	0.2	0.3	0.4	0.5	0.6	0.7
Fully-supervised	Wang et al. [35]	18.2	17.0	14.0	11.7	8.3	-	-
	Oneata et al. [23]	36.6	33.6	27.0	20.8	14.4	-	-
	Shou et al. [27]	47.7	43.5	36.3	28.7	19.0	10.3	5.3
	SST [3]	-	-	37.8	-	23.0	-	-
	CDC [25]	-	-	40.1	29.4	23.3	13.1	7.9
	Dai et al. [6]	-	-	-	33.3	25.6	15.9	9.0
	R-C3D [36]	54.5	51.5	44.8	35.6	28.9	-	-
	Gao et al. [9]	-	-	50.1	41.3	31.0	19.1	9.9
	SSN [44]	66.0	59.4	51.9	41.0	29.8	19.6	10.7
	TAL-Net [5]	59.8	57.1	53.2	48.5	42.8	33.8	20.8
	Alwassel et al. [1]	-	-	51.8	42.4	30.8	20.2	11.1
	BSN [16]	-	-	53.5	45.0	36.9	28.4	20.0
Weakly-supervised	Sun et al. [30]	-	-	8.5	-	4.4	-	-
	Hide [28]	36.4	27.8	19.5	12.7	6.8	-	-
	UntrimmedNets [33]	44.4	37.7	28.2	21.1	13.7	-	-
	STPN [21]	52.0	44.7	35.5	25.8	16.9	9.9	4.3
	Autoloc [26]	-	-	35.8	29.0	21.2	13.4	5.8
	W-TALC [24]	55.2	49.6	40.1	31.1	22.8	-	7.6
	Liu et al. [18]	-	-	37.0	30.9	23.9	13.9	7.1
	Yu et al. [37]	-	-	39.5	-	24.5	-	7.1
	3C-Net [20]	59.1	53.5	44.2	34.1	26.6	-	8.1
	Nguyen et al. [22]	64.2	59.5	49.1	38.4	27.5	17.3	8.6
EM-MIL (ours)	59.1	52.7	45.5	36.8	30.5	22.7	16.4	

Then we raise the learning rate to 4 times larger and decrease the alternating cycle to 1 epoch for another 35 epoch. For ActivityNet1.2 dataset, we use a similar training approach but the alternating cycle is 5 epochs and the learning rate is constant. We use our model to generate instance assignment Q_t and classification score $P_{t,c}$ separately for RGB and Flow branch. Then, we fuse the RGB/Flow score by weighted averaging them. The threshold hyper-parameter γ in Eq. 5 is set to 0.15 for THUMOS14 dataset and 0 for ActivityNet1.2 dataset. Intuitively, γ implies a distribution prior about how similar the same action is across several videos. The size of γ should be negatively correlated with the variance of the action’s feature distribution.

4.2 Comparison with State-of-the-art Approaches

Results on THUMOS14 Dataset: We compare our model’s results on the THUMOS14 dataset with state-of-the-art results in Table 1. Our model outperforms all the previous published models and achieves a new state-of-the-art result at mAP@0.5, **30.5%**. This result is achieved with simple EM training and

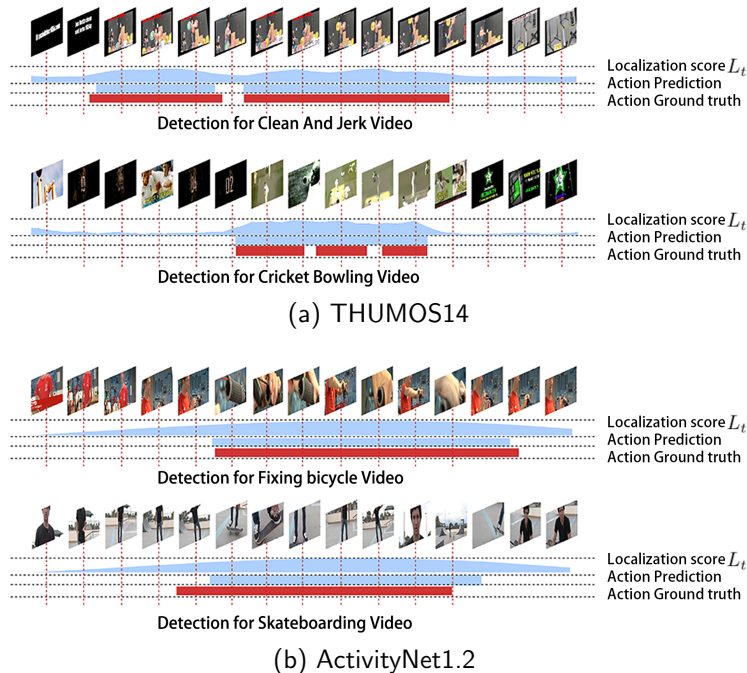


Fig. 5: Qualitative visualization of the predicted activities by our EM-MIL model (best viewed in color). (a) and (b) show results for two videos each on THUMOS14 and ActivityNet1.2, one good prediction example (top) and one bad prediction (bottom). Ground truth activity segments are marked in red. Localization score distribution L_t and predicted activity segments are in blue.

the pseudo-labeling scheme, without auxiliary losses to regularize the learning process. Notably while some models like untrimmedNets [33] use a different backbone (TSN and TCN), most recent models [18,37,20,22] use the same two-stream I3D feature extraction backbone as our model does, thus are fair comparison from the feature extraction aspect. Compared to the best result among the four recent models [18,37,20,22], we get 3% significant improvement at mAP@0.5. Our model also shows more significant improvement at higher threshold metrics tIoU=0.6 and tIoU=0.7, which implies our action proposals are more complete. On the other hand, our performance is slightly worse in the low IoU metrics.

Several examples’ qualitative results are shown in Figure 5(a). For each example, we show the video, intermediate score map L_t from our model, final activity detection result and ground truth temporal segment annotations. In the first example of “Clean and Jerk”, we localize the activity correctly with almost 100% overlap. We also show one bad localized example in the second example, in which our model overestimates the “Cricket Bowling” activity duration by 20%, as an effect of the interactive shrinkage training process which at first labels every instance positive. Our model greatly resolves the incompleteness problem

Table 2: Our EM-MIL detection results on ActivityNet1.2 in terms of mAP@{0.5, 0.7, 0.9} and average mAP at tIoU thresholds $\alpha \in (0.5, 0.95)$ with step 0.05 (in percentage). The top half of the table shows fully-supervised methods while the bottom for weakly-supervised ones.

	Models	α			avg. mAP
		0.5	0.7	0.9	
Fully	SSN [44]	41.3	30.4	13.2	26.6
Weakly	Untrim. [33]	7.4	3.9	1.2	3.6
	Autoloc [26]	27.3	17.5	6.8	16.0
	W-TALC [24]	37.0	14.6	4.2	18.0
	3C-Net [20]	37.2	23.7	9.2	21.7
	Liu et al. [18]	37.1	23.4	9.2	21.6
	TSM [37]	28.3	18.9	7.5	17.1
	EM-MIL (ours)	37.4	23.1	2.0	20.3

for the activity detection in videos containing multiple action segments, while in some cases it might also bring in additional false positives.

Results on ActivityNet1.2 Dataset: We compare our model’s results on the ActivityNet1.2 dataset with state-of-the-art results in Table 2. Our model outperforms previously published models in mAP@0.5 and gets the value of **37.4%**. Despite the state-of-the-art result in mAP@0.5, when compared to previous models [24,20,18] our model performs worse in high tIoU metrics, which is the opposite to what we observed on THUMOS14 dataset, that our model outperforms theirs on high tIoU thresholds by a large margin. We further investigate the different result trends on both datasets. Videos in the THUMOS14 dataset contains multiple action segments, each segment with relatively short duration. It has high localization requirement where our model outperforms pervious ones at high tIoU. Unlike THUMOS14, most (> 99%) videos in the ActivityNet1.2 dataset have only one action class, and most of these videos have few activity segments which compose a big portion of the whole video duration. Thus videos in ActivityNet1.2 dataset can be regarded as trimmed actions in certain extent. As a result, we speculate that the action localization performance in the ActivityNet1.2 dataset depends more on the classification module, which might be the bottleneck for our model.

This speculation also correlates with the different λ settings in formula 9 when calculating localization score on THUMOS14 and ActivityNet1.2 datasets. According to our model’s assumption, key instance assignment score Q_t implies the action localization regions and higher weight for this part facilitates the localization process. On THUMOS14, the weight λ for the key instance assignment score Q_t is set to a high value 0.8. But for ActivityNet1.2, the classification score $P_{t,c}$ has a higher weight (0.7), implying that to succeed on this dataset the model mostly relies on classification. For further illustration, we also visualize some good and bad detection results from ActivityNet1.2 dataset in Figure 5(b).

Table 3: Ablation results for the pseudo labeling and EM alternating training on THUMOS14 dataset in terms of mAP@0.5 (%).

Ablation Models	Pseudo Label	Alternating Training	mAP@0.5
Alternating model		✓	24.5
Pseudo labeling model	✓		26.8
Full Model	✓	✓	30.5

4.3 Ablation Studies

We ablate our proposed pseudo label generation scheme and the Expectation-Maximization alternating training method on THUMOS14 dataset, and mAP@0.5 results are shown in Table 3.

Ablation on the Pseudo Labeling: We first ablate on the pseudo labeling scheme for $\hat{z}_t \hat{y}_{t,c}$, and include the results in Table 3. In this ablation, we switch our learning to be supervised by a normal attention MIL loss based on softmax function, similar to the case in [33,21]. In the E step, classification scores of all classes contribute collectively to the attention weights. In the M step, attention weights are applied equally to both positive and negative videos without paying special attention to the label of the bag. In Table 3, compared to the “Alternating model” doing alternating training but with a normal attention, “Full Model” improves mAP@0.5 from 24.5% to 30.5%, which is 6% absolute improvement. This indicates the usefulness of the proposed pseudo labeling strategy. It models the key instance assignment explicitly as hidden variables and aligns with the MIL assumption better.

Ablation on the EM Alternating Training Technique: We also evaluate the effectiveness of Expectation-Maximization alternating training technique compared to joint optimization. The EM training method iteratively estimates the key instance assignment, then maximizes the video classification accuracy, and achieves better activity detection performance. In Table 3, “Full Model” improves mAP@0.5 from 26.8% to 30.5% compared to the “Pseudo labeling” model. The 4% significant result gain indicates the effectiveness of the alternating training technique. The same training process can be potentially applied on other MIL based models for weakly-supervised object detection task to improve accuracy.

5 Conclusion

The EM-MIL framework from the traditional MIL learning is under-explored in deep learning settings. By allowing us to explicitly model latent variables, this framework improves our control over the learning objective, which leads to state of the art performance. While this work uses a relatively simple pseudo-labeling method, it can easily be extended to do more precise sampling, inference and estimation through modeling the latent distribution. Incorporating the temporal constraints and regularization methods used in contemporary works is a promising direction for further performance improvements.

References

1. Alwassel, H., Caba Heilbron, F., Ghanem, B.: Action search: Spotting actions in videos and its application to temporal action localization. In: Proceedings of the European Conference on Computer Vision (ECCV). pp. 251–266 (2018) [11](#)
2. Alwassel, H., Heilbron, F.C., Thabet, A., Ghanem, B.: Refinoloc: Iterative refinement for weakly-supervised action localization. arXiv preprint arXiv:1904.00227 (2019) [5](#)
3. Buch, S., Escorcia, V., Shen, C., Ghanem, B., Carlos Niebles, J.: Sst: Single-stream temporal action proposals. In: Proceedings of the IEEE conference on Computer Vision and Pattern Recognition. pp. 2911–2920 (2017) [11](#)
4. Carreira, J., Zisserman, A.: Quo vadis, action recognition? a new model and the kinetics dataset. 2017 IEEE Conference on Computer Vision and Pattern Recognition (CVPR) pp. 4724–4733 (2017) [10](#)
5. Chao, Y.W., Vijayanarasimhan, S., Seybold, B., Ross, D.A., Deng, J., Sukthankar, R.: Rethinking the faster r-cnn architecture for temporal action localization. In: Proceedings of the IEEE Conference on Computer Vision and Pattern Recognition. pp. 1130–1139 (2018) [11](#)
6. Dai, X., Singh, B., Zhang, G., Davis, L.S., Qiu Chen, Y.: Temporal context network for activity localization in videos. In: Proceedings of the IEEE International Conference on Computer Vision. pp. 5793–5802 (2017) [11](#)
7. Dietterich, T., Lathrop, R., Lozano-Perez, T.: Solving the multiple instance problem with axis-parallel rectangles. In: Artificial Intelligence. vol. 89, pp. 31–71 (1997) [2](#), [3](#), [5](#)
8. Dooly, D.R., Zhang, Q., Goldman, S.A., Amar, R.A., Brodley, E., Danyluk, A.: Multiple-instance learning of real-valued data. In: Journal of Machine Learning Research. pp. 3–10. Morgan Kaufmann (2001) [3](#), [5](#)
9. Gao, J., Yang, Z., Nevatia, R.: Cascaded boundary regression for temporal action detection. arXiv preprint arXiv:1705.01180 (2017) [11](#)
10. Heidarinvinch, F., Mirmehdi, M., Damen, D.: Weakly-supervised completion moment detection using temporal attention. In: The IEEE International Conference on Computer Vision (ICCV) Workshops (Oct 2019) [1](#)
11. Heilbron, F.C., Escorcia, V., Ghanem, B., Niebles, J.C.: ActivityNet: A Large-Scale Video Benchmark for Human Activity Understanding. In: IEEE Conference on Computer Vision and Pattern Recognition. pp. 961–970 (2015) [10](#)
12. Ilse, M., Tomczak, J.M., Welling, M.: Attention-based deep multiple instance learning. arXiv preprint arXiv:1802.04712 (2018) [2](#), [4](#), [6](#), [8](#)
13. Jiang, Y.G., Liu, J., Zamir, A.R., Toderici, G., Laptev, I., Shah, M., Sukthankar, R.: THUMOS Challenge: Action Recognition with a Large Number of Classes. <http://crcv.ucf.edu/THUMOS14/> (2014) [10](#)
14. Keeler, J.D., Rumelhart, D.E., Leow, W.K.: Integrated segmentation and recognition of hand-printed numerals. In: Lippmann, R.P., Moody, J.E., Touretzky, D.S. (eds.) Advances in Neural Information Processing Systems 3, pp. 557–563. Morgan-Kaufmann (1991) [5](#)
15. Li, X., Kan, M., Shan, S., Chen, X.: Weakly supervised object detection with segmentation collaboration. In: The IEEE International Conference on Computer Vision (ICCV) (October 2019) [2](#)
16. Lin, T., Zhao, X., Su, H., Wang, C., Yang, M.: Bsn: Boundary sensitive network for temporal action proposal generation. In: Proceedings of the European Conference on Computer Vision (ECCV). pp. 3–19 (2018) [11](#)

17. Liu, D., Jiang, T., Wang, Y.: Completeness modeling and context separation for weakly supervised temporal action localization. In: Proceedings of the IEEE Conference on Computer Vision and Pattern Recognition. pp. 1298–1307 (2019) [2](#), [3](#), [5](#)
18. Liu, Z., Wang, L., Zhang, Q., Gao, Z., Niu, Z., Zheng, N., Hua, G.: Weakly supervised temporal action localization through contrast based evaluation networks. In: Proceedings of the IEEE International Conference on Computer Vision. pp. 3899–3908 (2019) [5](#), [11](#), [12](#), [13](#)
19. Maron, O., Lozano-Pérez, T.: A framework for multiple-instance learning. In: Jordan, M.I., Kearns, M.J., Solla, S.A. (eds.) Advances in Neural Information Processing Systems 10, pp. 570–576. MIT Press (1998) [5](#)
20. Narayan, S., Cholakkal, H., Khan, F.S., Shao, L.: 3c-net: Category count and center loss for weakly-supervised action localization. In: Proceedings of the IEEE International Conference on Computer Vision. pp. 8679–8687 (2019) [2](#), [11](#), [12](#), [13](#)
21. Nguyen, P., Liu, T., Prasad, G., Han, B.: Weakly supervised action localization by sparse temporal pooling network. In: Proceedings of the IEEE Conference on Computer Vision and Pattern Recognition. pp. 6752–6761 (2018) [2](#), [4](#), [5](#), [6](#), [11](#), [14](#)
22. Nguyen, P.X., Ramanan, D., Fowlkes, C.C.: Weakly-supervised action localization with background modeling. In: Proceedings of the IEEE International Conference on Computer Vision. pp. 5502–5511 (2019) [2](#), [6](#), [11](#), [12](#)
23. Oneata, D., Verbeek, J., Schmid, C.: The LEAR submission at Thumos 2014. ECCV THUMOS Workshop (2014) [11](#)
24. Paul, S., Roy, S., Roy-Chowdhury, A.K.: W-talc: Weakly-supervised temporal activity localization and classification. In: Proceedings of the European Conference on Computer Vision (ECCV). pp. 563–579 (2018) [2](#), [3](#), [4](#), [9](#), [11](#), [13](#)
25. Shou, Z., Chan, J., Zareian, A., Miyazawa, K., Chang, S.F.: Cdc: Convolutional-de-convolutional networks for precise temporal action localization in untrimmed videos. In: Proceedings of the IEEE Conference on Computer Vision and Pattern Recognition. pp. 5734–5743 (2017) [11](#)
26. Shou, Z., Gao, H., Zhang, L., Miyazawa, K., Chang, S.F.: Autoloc: Weakly-supervised temporal action localization in untrimmed videos. In: Proceedings of the European Conference on Computer Vision (ECCV). pp. 154–171 (2018) [5](#), [9](#), [11](#), [13](#)
27. Shou, Z., Wang, D., Chang, S.F.: Temporal Action Localization in Untrimmed Videos via Multi-stage CNNs. In: IEEE Conference on Computer Vision and Pattern Recognition (2016) [11](#)
28. Singh, K.K., Lee, Y.J.: Hide-and-peek: Forcing a network to be meticulous for weakly-supervised object and action localization. In: 2017 IEEE International Conference on Computer Vision (ICCV). pp. 3544–3553. IEEE (2017) [5](#), [11](#)
29. Su, H., Zhao, X., Lin, T.: Cascaded pyramid mining network for weakly supervised temporal action localization. In: Asian Conference on Computer Vision. pp. 558–574. Springer (2018) [5](#)
30. Sun, C., Shetty, S., Sukthankar, R., Nevatia, R.: Temporal localization of fine-grained actions in videos by domain transfer from web images. In: Proceedings of the 23rd ACM international conference on Multimedia. pp. 371–380. ACM (2015) [11](#)
31. Tang, P., Wang, X., Bai, X., Liu, W.: Multiple instance detection network with online instance classifier refinement. In: Proceedings of the IEEE Conference on Computer Vision and Pattern Recognition. pp. 2843–2851 (2017) [5](#)

32. Wan, F., Liu, C., Ke, W., Ji, X., Jiao, J., Ye, Q.: C-mil: Continuation multiple instance learning for weakly supervised object detection. In: CVPR. pp. 2199–2208 (2019) [2](#)
33. Wang, L., Xiong, Y., Lin, D., Van Gool, L.: Untrimmednets for weakly supervised action recognition and detection. In: Proceedings of the IEEE conference on Computer Vision and Pattern Recognition. pp. 4325–4334 (2017) [2](#), [4](#), [5](#), [9](#), [11](#), [12](#), [13](#), [14](#)
34. Wang, L., Xiong, Y., Wang, Z., Qiao, Y., Lin, D., Tang, X., Van Gool, L.: Temporal segment networks: Towards good practices for deep action recognition. In: European conference on computer vision. pp. 20–36. Springer (2016) [10](#)
35. Wang, L., Yu Qiao, Y., Tang, X.: Action Recognition and Detection by Combining Motion and Appearance Features. ECCV THUMOS Workshop **1** (2014) [11](#)
36. Xu, H., Das, A., Saenko, K.: R-c3d: Region convolutional 3d network for temporal activity detection. In: Proceedings of the IEEE international conference on computer vision. pp. 5783–5792 (2017) [11](#)
37. Yu, T., Ren, Z., Li, Y., Yan, E., Xu, N., Yuan, J.: Temporal structure mining for weakly supervised action detection. In: Proceedings of the IEEE International Conference on Computer Vision. pp. 5522–5531 (2019) [11](#), [12](#), [13](#)
38. Yuan, Y., Lyu, Y., Shen, X., Tsang, I.W., Yeung, D.Y.: Marginalized average attentional network for weakly-supervised learning. arXiv preprint arXiv:1905.08586 (2019) [2](#), [3](#), [5](#)
39. Zach, C., Pock, T., Bischof, H.: A duality based approach for realtime tv-l 1 optical flow. In: Joint pattern recognition symposium. pp. 214–223. Springer (2007) [10](#)
40. Zeng, R., Gan, C., Chen, P., Huang, W., Wu, Q., Tan, M.: Breaking winner-takes-all: Iterative-winners-out networks for weakly supervised temporal action localization. IEEE Transactions on Image Processing **28**(12), 5797–5808 (2019) [5](#)
41. Zhang, C., Platt, J.C., Viola, P.A.: Multiple instance boosting for object detection. In: Weiss, Y., Schölkopf, B., Platt, J.C. (eds.) Advances in Neural Information Processing Systems 18, pp. 1417–1424. MIT Press (2006) [5](#)
42. Zhang, Q., Goldman, S.A.: Em-dd: An improved multiple-instance learning technique. In: Dietterich, T.G., Becker, S., Ghahramani, Z. (eds.) Advances in Neural Information Processing Systems 14, pp. 1073–1080. MIT Press (2002), <http://papers.nips.cc/paper/1959-em-dd-an-improved-multiple-instance-learning-technique.pdf> [3](#), [5](#)
43. Zhang, Q., Goldman, S.A.: Em-dd: An improved multiple-instance learning technique. In: Advances in neural information processing systems. pp. 1073–1080 (2002) [6](#)
44. Zhao, Y., Xiong, Y., Wang, L., Wu, Z., Tang, X., Lin, D.: Temporal action detection with structured segment networks. In: Proceedings of the IEEE International Conference on Computer Vision. pp. 2914–2923 (2017) [11](#), [13](#)
45. Zhong, J.X., Li, N., Kong, W., Zhang, T., Li, T.H., Li, G.: Step-by-step erasing, one-by-one collection: A weakly supervised temporal action detector. arXiv preprint arXiv:1807.02929 (2018) [5](#)